Neurobiology of Disease

Impaired Feedforward Inhibition of the Thalamocortical Projection in Epileptic Ca^{2+} Channel Mutant Mice, *tottering*

Sachie Sasaki,[1,2] Kadrul Huda,[1] Tsuyoshi Inoue,[1,2] Mariko Miyata,[1,2] and Keiji Imoto[1,2]

[1]Department of Information Physiology, National Institute for Physiological Sciences, and [2]School of Life Sciences, The Graduate University for Advanced Studies, Okazaki 444-8787, Japan

The *tottering* (*tg*) mice have a mutation in the $Ca_V2.1$ (P/Q-type) voltage-dependent Ca^{2+} channel $\alpha_1 2.1$ subunit gene. *tg* mice show not only cerebellar ataxia but also absence epilepsy, which begins at ~3 weeks of age and persists throughout life. Similarities in EEG and sensitivity to antiepileptic drugs suggest that *tg* mice are a good model for human absence epilepsy. Although imbalance between excitatory and inhibitory activity in the thalamocortical network is thought to contribute to the pathogenesis of absence epilepsy, the effect of the mutation on thalamocortical synaptic responses remains unknown. Here we showed imbalanced impairment of inhibitory synaptic responses in *tg* mice using brain slice preparations. Somatosensory thalamocortical projection makes not only monosynaptic glutamatergic connections but also disynaptic GABAergic connections, which mediate feedforward inhibition, onto layer IV neurons. In *tg* mice, IPSC amplitudes recorded from layer IV pyramidal cells of the somatosensory cortex in response to thalamic stimulation became disproportionately reduced compared with EPSC amplitudes at later developmental stages (postnatal days 21–30). Similar results were obtained by local stimulation of layer IV pyramidal neurons. However, IPSC reduction was not seen in layer V pyramidal neurons of epileptic *tg* mice or in layer IV pyramidal neurons of younger *tg* mice before the onset of epilepsy (postnatal days 14–16). These results showed that the feedforward inhibition from the thalamus to layer IV neurons of the somatosensory cortex was severely impaired in *tg* mice and that the impairment of the inhibitory synaptic transmission was correlated to the onset of absence epilepsy.

Key words: **absence seizure; thalamocortical projection; feedforward inhibition; synaptic transmission; Ca^{2+} channel; mutant mice**

Introduction

Absence seizure is one type of generalized epilepsy. It is characterized by bilaterally synchronous spike-and-wave discharges (SWDs) in the electroencephalogram (EEG) over wide cortical areas. The generalized nature of the SWDs led to the hypothesis of a common central pacemaker and implied the thalamic contribution to the absence seizure (Jasper and Kershman, 1941). Conversely, analyses of the penicillin-induced generalized epilepsy suggested the importance of intracortical processes in the SWDs (Avoli and Gloor, 1982). Because the thalamus can generate strong synchronized oscillatory activities through interaction between thalamocortical relay cells and cells of the reticular thalamic nucleus (Steriade et al., 1993), these results, combined together, led to the hypothesis that an aberration of the interplay between the cerebral cortex and the thalamus causes the SWDs. However, the relative contribution of the thalamus and the cerebral cortex to the pathophysiological condition has been a matter of severe debate for decades.

The homozygous *tottering* (*tg*) mice are an established genetic model of absence seizure (Noebels and Sidman, 1979). The *tg* mice have a mutation in the gene encoding the $\alpha_1 2.1$ subunit of the voltage-gated Ca^{2+} channel (Fletcher et al., 1996). The $\alpha_1 2.1$ subunit forms the channel pore of the $Ca_V2.1$ (P/Q-type) channel (Mori et al., 1991), which plays essential roles in a variety of functions, including neurotransmitter release at presynaptic sites (Wheeler et al., 1994). Extensive studies on mutated $Ca_V2.1$ channels in native neurons as well as in recombinant expression systems revealed that the *tg* mutation reduced the Ca^{2+} influx through the Ca^{2+} channel (Wakamori et al., 1998; Qian and Noebels, 2000). In the thalamocortical loop, excitatory but not inhibitory synaptic transmission was reduced in the somatosensory thalamus of *tg* mice (Caddick et al., 1999). However, synaptic transmission from the thalamus to the cortex was not examined in *tg* mice or other epileptic model animals.

In this study, we examined excitatory and inhibitory synaptic responses in layer IV pyramidal neurons in response to thalamic and cortical stimulation using somatosensory thalamocortical brain slice preparations. The results indicated that the mutation of $Ca_V2.1$ calcium channel in *tg* mice results in a significant impairment of inhibitory, but not excitatory, synaptic transmission to layer IV pyramidal neurons in *tg* mice over 3 weeks of age. The impairment resulted in dysfunction of feedforward inhibition, which, in wild-type (wt) mice, suppressed excitability of layer IV neurons in response to thalamocortical inputs. The defective feedforward inhibition may play a role in the pathogenesis of absence epilepsy.

Received Jan. 18, 2005; revised Jan. 29, 2006; accepted Jan. 30, 2006.

This work is supported in part by research grants from the Ministry of Education, Culture, Sports, Science, and Technology.

Correspondence should be addressed to Keiji Imoto, Department of Information Physiology, National Institute for Physiological Sciences, Myodaiji, Okazaki 444-8787, Japan. E-mail: keiji@nips.ac.jp.

K. Huda's present address: Waseda-Olympus Bioscience Research Institute, Singapore 138667, Singapore.

DOI:10.1523/JNEUROSCI.5422-05.2006

 0270-6474/06/263056-10$15.00/0

Parts of this work have been published previously in abstract form (Huda and Imoto, 2001).

Materials and Methods

Animals. The C57BL/6-*tg* strain of *tg* mice was introduced from The Jackson Laboratory (Bar Harbor, ME). Mice at postnatal day 14 (P14) to P30 were used for the experiments. Mice were provided with a commercial diet (CE-2; Nihon Clea, Tokyo, Japan) and water *ad libitum* under conventional conditions with controlled temperature, humidity, and lighting (22 ± 2°C, 55 ± 5%, and 12 h light/dark cycle with lights on at 6:00 A.M.). The strain was maintained and propagated by mating between heterozygous mice. All animal studies described herein were reviewed and approved by the ethical committee in our institute and were performed according to the institutional guidelines concerning the care and handling of experimental animals.

Genotyping of tg *mice.* Genomic DNA was extracted from the tail. The genomic region encoding a part of the Ca^{2+} channel $\alpha_1$2.1 subunit gene was amplified using the cDNA Polymerase Mix (Clontech, Palo Alto, CA) and two sets of PCR primers, which were 5′-TTAATTTTG-ATGAAGGGACTCC-3′ (sense for wt), 5′-TTAATTTTGATGAAGG-GACTCT-3′ (sense for *tg*), and 5′-CCAGCAACAATGAAAACAAGC-ATTCCAAAACAGC-3′ (antisense for both). The DNA-extract solution (2 μl) was used as a template for PCR (28 cycles of 94°C for 30 s, 55°C for 30 s, and 72°C for 30 s, and final extension at 72°C for 7 min). The resulting PCR products were subjected to electrophoresis on a 2.0% agarose gel.

Slice preparation. Somatosensory thalamocortical slices were prepared as described by Agmon and Connors (1991). Auditory thalamocortical slices were prepared as described by Cruikshank et al. (2002). Mice were killed by decapitation under deep halothane general anesthesia. Brains were removed and put into ice-cold cutting solution containing the following (in mM): 120 choline-Cl, 3 KCl, 1.25 NaH_2PO_4, 28 $NaHCO_3$, 8 $MgCl_2$, and 22 glucose, saturated with carbogene (95% O_2 and 5% CO_2). The tissue was cut into 450-μm-thick slices with a vibratome (VT1000S; Leica, Nussloch, Germany). These slices were then incubated at 32°C for 30 min and room temperature for at least 30 min in artificial CSF (ACSF) containing the following (in mM): 125 NaCl, 25 $NaHCO_3$, 25 glucose, 2.5 KCl, 1.25 NaH_2PO_4, 2 $CaCl_2$, and 1 $MgCl_2$, bubbled with carbogene.

To minimize artifactual effect of severing axons during the slicing procedure, we only used somatosensory thalamocortical slices in which thalamic stimulation evoked >100 pA EPSCs (10 mA intensity) in voltage-clamp mode or >1 mV EPSPs (50 μA intensity) in current-clamp mode.

Electrophysiological recordings. A whole-cell voltage-clamp recording was made from layer IV and V pyramidal neurons of the mouse barrel cortex, which were visually identified using an upright microscope equipped with a 60× water immersion objective (BX51WI; Olympus Optical, Tokyo, Japan) and an infrared differential interference contrast (DIC) video system (C2400–79H; Hamamatsu Photonics, Hamamatsu, Japan). Patch pipettes were made from borosilicate capillaries (2.0 mm outer diameter and 1.0 mm inner diameter; Hilgenberg, Malsfeld, Germany). EPSCs and IPSCs were recorded with an EPC9 patch-clamp amplifier (HEKA Elektronik, Lambrecht, Germany). The access resistance for recording was <15 MΩ and compensated by 50–70%. Capacitance of recorded cells was not significantly different between wt and *tg* mice (61.3 ± 7.9 pF for wt, $n = 12$; 55.6 ± 9.5 pF for *tg*, $n = 11$; $p > 0.05$). Cells were rejected if access resistance increased above 15 MΩ. Biocytin at 0.5% (Sigma, St. Louis, MO) was included in internal solutions for morphological characterization of recorded neurons. Stimulation and data acquisition were performed using the PULSE program (version 8.54; HEKA Elektronik). The current signals were filtered at 3 kHz and digitized at 20 kHz. All electrophysiological recordings were performed at a bath temperature of 32°C.

Thalamocortical responses. Thalamocortical EPSCs and IPSCs were evoked by electrical stimulation (10 mA, 200 μs), using a stimulus isolator (ISO-FLEX; A.M.P.I., Jerusalem, Israel) and stainless steel bipolar semi-microelectrodes (A-M Systems, Carlsborg, WA) placed in the ventrobasal thalamic nucleus or the internal capsule (IC) (see Fig. 1*A*). Patch pipettes (3–6 MΩ) were filled with an internal solution containing the following (in mM): 140 Cs-CH_3SO_3, 5 KCl, 10 EGTA, 10 HEPES, 3 Mg-ATP, and 0.4 Na-GTP, adjusted to pH 7.4 with CsOH. QX-314 [*N*-(2,6-dimethylphenylcarbamoylmethyl)trimethylammonium bromide] (final concentration of 5 mM) was added to prevent Na^+ spike generation. DL-2-Amino-5-phosphonopentanoic acid (APV) (100 μM) was added to the external solution to block NMDA receptor-mediated currents, which otherwise often masked IPSCs. EPSCs were recorded at a holding potential (V_h) of −60 mV, whereas IPSCs were recorded at V_h of 0 mV. To obtain reversal potentials, AMPA receptor-mediated currents were recorded in response to pressure application of 5 mM AMPA (5–15 psi, 5–10 ms square pulse generated by PV830; World Precision Instruments, Sarasota, FL) in the presence of 1 μM tetrodotoxin (TTX) and 10 μM cyclothiazide, whereas $GABA_A$ receptor-mediated currents were recorded by local stimulation in the presence of 10 μM 6-cyano-7-nitroquinoxaline-2,3-dione (CNQX) and 100 μM APV. The reversal potential was determined by fitting the current–voltage plot by a linear regression ($r \geq 0.95$). The reversal potentials (V_{rev}) of AMPA receptor-mediated or $GABA_A$ receptor-mediated currents were +6.0 ± 1.4 mV ($n = 4$) and −64.4 ± 2.9 mV ($n = 3$), respectively. The conductance (G) was determined using the equation $G = I/(V_h - V_{rev})$, where I is EPSC or IPSC amplitude. Although excitatory and inhibitory thalamocortical responses were recorded in layer V pyramidal cells, we did not include the layer V thalamocortical responses, because the probability of the connection was low (Gil and Amitai, 1996).

Local responses. IPSCs and EPSCs were recorded at a holding potential of −60 mV in response to local electrical stimulation (0.1–10 mA, 200 μs) using a bipolar tungsten microelectrode with an intertip distance of 100 μm. The stimulation electrode was usually placed at ~100 μm from the soma of the recorded neuron. The resistance of patch pipettes was 3–6 MΩ when filled with intracellular solution. The internal solution for IPSCs contained the following (in mM): 140 CsCl, 9 NaCl, 1 EGTA, 10 HEPES, and 2 Mg-ATP, adjusted to pH 7.3 with CsOH. The internal solution for EPSCs contained the following (in mM): 115 K-gluconate, 20 KCl, 1 EGTA, 10 HEPES, 4 Mg-ATP, 0.3 Na-GTP, and 10 phosphocreatine, adjusted to pH 7.4 with KOH. QX-314 (final concentration of 5 mM) was added to prevent Na^+ spike generation. IPSCs and EPSCs were recorded in the presence of 10 μM CNQX plus 100 μM APV and 10 μM (−)-bicuculline methochloride (bicuculline), respectively. Bicuculline blockade (10 μM) did not lead to epileptic activities, presumably because there remained some inhibitory synaptic activities in thick slice preparations (450 μm) preventing abnormal discharges.

Miniature IPSCs. For recording miniature IPSCs (mIPSCs), slices from P21–P27 wt and *tg* mice were bathed in ACSF containing 1 μM TTX, 10 μM CNQX, and 100 μM APV. The internal solution was the same as used for IPSC measurement. The holding potential was −60 mV. Currents were filtered at 3 kHz and digitized at 20 kHz. Series resistance was measured periodically. Off-line data analyses were performed with an IgorPro program (WaveMetrics, Lake Oswego, OR). Data were pooled from seven neurons (400 consecutive events each, $n = 2800$).

Current-clamp recoding. Current-clamp recordings were obtained in bridge mode of an Axoclamp 2B amplifier (Molecular Devices, Palo Alto, CA). Patch pipettes (3–6 MΩ) were filled with an internal solution containing the following (in mM): 135 K-CH_3SO_3, 6 NaCl, 0.2 EGTA, 10 HEPES, 4 Mg-ATP, 0.3 Na-GTP, and 10 phosphocreatine, adjusted to pH 7.3 with KOH. The series resistances were compensated with the bridge balance. Only cells that had resting membrane potentials more hyperpolarized than −50 mV and showed overshooting action potentials were accepted for this study. Electrical signals were filtered at 3 kHz and then digitized at 10 kHz using the ITC-16 interface (InstruTech, Port Washington, NY). Thalamocortical postsynaptic potentials (PSPs) in layer IV pyramidal cells were evoked by electrical stimulation (0.05–0.4 mA, 200 μs) using a bipolar tungsten microelectrode with an intertip distance of 250 μm placed in the internal capsule. In recordings of the thalamocortical PSPs, the membrane potential of layer IV pyramidal cells was set to −60 mV by current injection. The reversal potential of chloride currents, estimated by Nernst equation, is −81.6 mV under the condition of our current-clamp recordings.

Histological procedure. For immunohistochemistry, wt and *tg* mice aged P21–P23 were anesthetized with 75 mg/kg pentobarbital and per-

fused intracardially with 4% paraformaldehyde and 0.2% picric acid in 0.1 M sodium phosphate buffer (PB) for 12 min. Brains were removed and fixed overnight at 4°C and subsequently incubated in PB containing 10, 20, and 30% sucrose for overnight each. The tissue was sliced at 40 μm along the coronal section by a microtome (SM2000R; Leica). Tissue slices were washed in 0.05 M Tris-buffered saline (TBS) before incubation in 1% H_2O_2 for 1 h. Slices were washed three times in TBS and incubated with a rabbit polyclonal antibody against glutamic acid decarboxylase (GAD) (1:5000; Chemicon, Temecula, CA) in TBS containing 10% normal goat serum and 2% bovine serum albumin for two overnights at 4°C. The tissues were washed three times in TBS and incubated 3 h at room temperature in biotinylated anti-rabbit IgG (Vector Laboratories, Burlingame, CA) using a 1:200 final dilution including normal goat serum and TBS. After rinses, the tissues were incubated with avidin–biotin–peroxidase complex (ABC Elite kit; Vector Laboratories) in TBS for 30 min. After washing in TBS, the tissues were reacted with DAB (0.05%) and H_2O_2 (0.002%) in TBS. They were then postfixed for 30 min in 1% OsO_4 in PB, dehydrated in graded ethanol, and flat embedded on glass slides in Epon. Immunostaining clearly stained the somata of GABAergic neurons, sparing their nuclei. The number of the stained cells was measured in at least 1-mm-wide vertical strips in layer IV barrel cortex (typically 300 μm height × 1000 μm width). To ascertain the barrel cortex, alternate sections were stained for Nissl and GAD.

Data analyses and statistics. Data analyses were performed using IgorPro. The values of IPSC and EPSC peak amplitudes were obtained from averages of 5–10 consecutive traces. All values are given as means ± SEMs. Statistical comparison between wt and *tg* mice was performed by *t* test (*$p < 0.05$, **$p < 0.01$) or by two-way repeated-measures ANOVA with *post hoc* Bonferroni's test. Distributions of mIPSC amplitude and interevent interval (IEI) were compared between wt and *tg* mice using Kolmogorov–Smirnov test. In all cases, significance was set at $p < 0.05$. Statistical analyses were performed using SPSS (SPSS, Chicago, IL).

Chemicals. Phosphocreatine, QX-314, CNQX, APV, and picrotoxin were obtained from Sigma. TTX was obtained from Sankyo (Tokyo, Japan). Bicuculline was obtained from Tocris Cookson (Avonmouth, UK). Peptide toxins ω-agatoxin IVA (ω-Aga-IVA) and ω-conotoxin GVIA (ω-CTx-GVIA) were obtained from Peptide Institute (Osaka, Japan). All other chemicals were from Nacalai Tesque (Kyoto, Japan) or Wako Pure Chemical Industries (Osaka, Japan). ω-Aga-IVA and ω-CTx-GVIA were coapplied with 1 mg/ml cytochrome *c* from horse heart (Nacalai Tesque) to prevent unspecific binding of the peptide toxins.

Results

Thalamocortical responses in adult wt and *tg* mice

In the somatosensory cortex, layer IV is the main gateway for afferent fibers originating in the respective thalamic relay nuclei (for review, see Douglas and Martin, 2004). The interplay between the cerebral cortex and the thalamus can be investigated using rodent thalamocortical brain slice preparations, which are unique in including both the ventrobasal nucleus of the thalamus and the somatosensory (barrel) cortex with the functional connectivity between them (Agmon and Connors, 1991). There are two major types of morphologically different excitatory neurons in layer IV: spiny stellate cells and pyramidal cells (Simons and Woolsey, 1984). Because it was technically easier to identify pyramidal cells in the slice preparation under the DIC video microscopy, we focused on layer IV pyramidal cells in this study so that a relatively homogenous neuronal population could be studied.

Voltage-clamp recordings were made from layer IV pyramidal cells of the barrel cortex in the whole-cell patch-clamp configuration (Fig. 1*A*). Most of the recorded neurons were examined morphologically by including biocytin in the pipette and staining after electrophysiological recordings. EPSCs and IPSCs evoked by thalamic stimulation were measured in the presence of the NMDA receptor antagonist APV (100 μM) and compared between wt and epileptic *tg* mice (P21–P30) (Fig. 1*B1*).

When the holding potential was −60 mV, prominent EPSCs were observed in layer IV pyramidal cells of wt and *tg* mice (Fig. 1*B1*, top traces). At the holding potential of 0 mV, EPSCs became very small and there appeared large outward currents in wt, whereas the current amplitude was much smaller in *tg* mice (Fig.

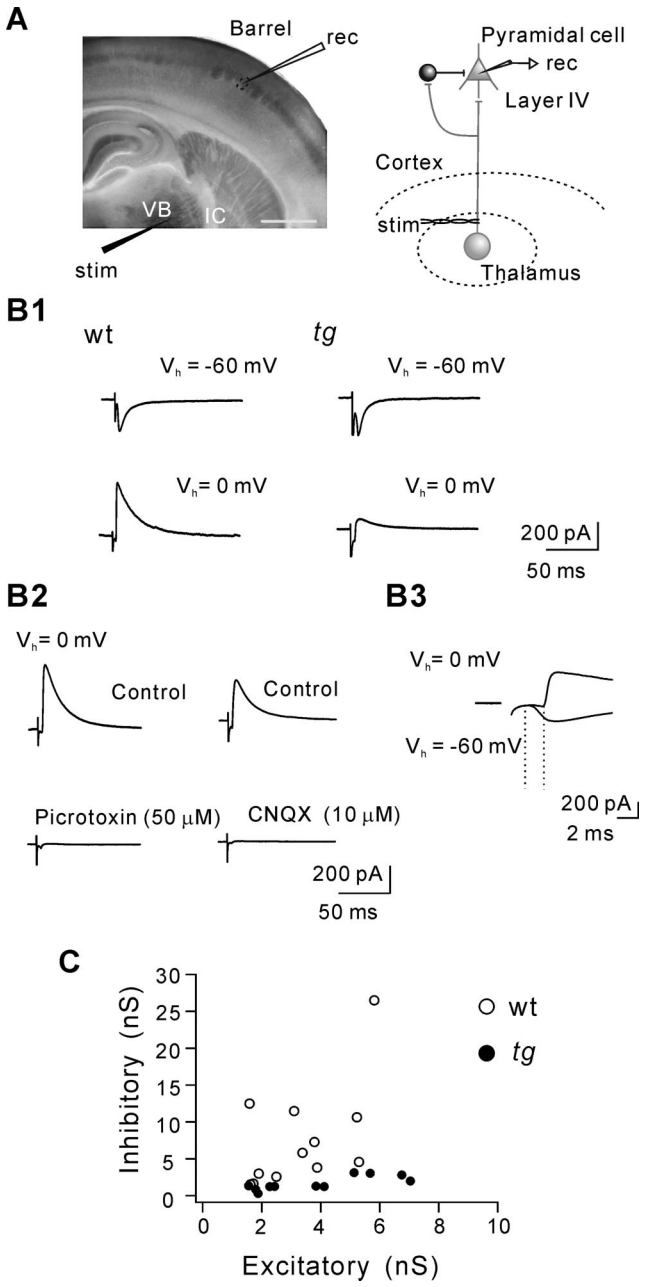

Figure 1. IPSCs and EPSCs recorded in layer IV pyramidal cells in response to thalamic stimulation. ***A***, Left, A thalamocortical brain slice preparation (cytochrome *c* oxidase staining). Scale bar, 1 mm. The black pointer indicates a typical position of stimulation. A barrel is indicated by a dotted circle. Recordings were made from neurons within a barrel. VB, Ventrobasal nucleus of the thalamus; IC, internal capsule. Right, The scheme of the thalamocortical circuit. ***B1***, Synaptic currents evoked by thalamic stimulation were recorded from layer IV pyramidal cells in wt and *tg* mice (P21–P30). EPSCs were recorded at a holding potential of −60 mV (top traces). When the holding potential was 0 mV, IPSCs became prominent (bottom traces). ***B2***, The outward currents at a holding potential of 0 mV were blocked by picrotoxin (50 μM) (left) and also abolished by CNQX (10 μM) (right). ***B3***, The IPSC and EPSC traces are superimposed in an expanded timescale (the same data used in ***B1*** for wt). The mean delay between the onset EPSC and IPSC was 1.3 ± 0.08 ms ($n = 12$) for wt and 1.4 ± 0.15 ms ($n = 11$) for *tg* mice. ***C***, The relationship between the excitatory and inhibitory conductances. Each point represents data from a single neuron.

1*B1*, bottom traces). The outward currents were $GABA_A$ receptor-mediated IPSCs, because they were completely blocked by the $GABA_A$ receptor antagonist picrotoxin (50 μM) (Fig. 1*B2*). Both EPSCs and IPSCs were completely abolished by the non-NMDA receptor antagonist CNQX (10 μM) (Fig. 1*B2*). Because the synaptic delay between the stimulation and the onset of EPSCs was short (2.1 ± 0.12 ms; $n = 12$), EPSCs were mainly monosynaptic responses. In contrast, the onset of IPSCs always followed the onset of EPSCs, with the mean delay between the onsets of EPSCs and IPSCs of 1.3 ± 0.08 ms ($n = 12$) (Fig. 1*B3*). Together with the CNQX sensitivity of IPSCs, these observations suggested that IPSCs were mediated by a disynaptic response, i.e., by inhibitory interneurons excited by excitatory thalamocortical inputs, forming a circuit of feedforward inhibition. The observation that layer IV pyramidal neurons receive strong feedforward inhibition was consistent with the previous reports (Agmon and Connors, 1992; Porter et al., 2001).

Figure 1*C* shows the relationship between the conductance values for EPSCs and IPSCs obtained from individual cells, in which the excitatory conductance ranged from 1 to ~8 nS in both wt and *tg* mice. The inhibitory conductance in wt became larger with increasing excitatory conductance, although the conductance values were quite variable. In contrast, the inhibitory conductance in *tg* mice was very small, even with a large excitatory conductance. The ratio of inhibitory conductance to excitatory conductance was significantly reduced in *tg* mice (2.34 ± 0.60 for wt, $n = 12$; 0.46 ± 0.06 for *tg*, $n = 11$; $^{**}p < 0.01$, *t* test). These results demonstrated that feedforward IPSCs disynaptically evoked by thalamic stimulation were disproportionately decreased in layer IV pyramidal cells of *tg* mice.

Locally evoked IPSCs and EPSCs

Thalamocortical responses recorded in layer IV pyramidal cells were composed of at least two components of monosynaptic EPSCs and disynaptic IPSCs. The lags of the synaptic onsets between two types of responses were short. Pharmacological blockade of EPSCs also abolished IPSCs. These facts made it difficult to evaluate synaptic currents quantitatively, especially IPSCs. To circumvent this problem, we measured IPSCs and EPSCs evoked by local stimulation within the somatosensory cortex. The stimulating electrode was placed at ~100 μm from the soma of the recorded pyramidal cells. IPSCs were recorded in the presence of CNQX (10 μM) and APV (100 μM), and EPSCs were recorded in the presence of bicuculline (10 μM). For measuring IPSCs, a pipette solution with a high chloride concentration was used so that IPSCs were observed as inward currents at a holding potential of −60 mV. IPSCs were blocked by bicuculline in both wt and *tg* mice (data not shown).

Local stimulation easily evoked large IPSCs in wt mice at P21–P30 (1079 ± 227 pA; $n = 10$, 1.0 mA stimulation) (Fig. 2*A*). In contrast, the IPSC amplitudes evoked by local stimulation were drastically reduced in *tg* mice at P21–P30 (145 ± 33 pA; $n = 10$, 1.0 mA stimulation). Statistical test using two-way repeated-measures ANOVA revealed a significant effect of the genotype ($F_{(1,18)} = 12.288$; $p < 0.004$) on IPSC amplitude. Additionally, there was a statistically significant interaction between stimulus intensity and genotype ($F_{(4,72)} = 7.484$; $p < 0.001$). *Post hoc* analyses using the Bonferroni's test revealed that the IPSC amplitudes were significantly smaller in *tg* than wt mice at stimulus intensities ≥0.8 mA [$^{*}p < 0.05$, $^{**}p < 0.01$ (Fig. 2*A*)]. Conversely, the EPSC amplitudes evoked by local stimulation increased with increment of stimulus intensity. Although EPSC amplitude appeared smaller in *tg* than wt mice (554 ± 96 pA, $n = 10$ in wt; 368 ± 88 pA, $n = 10$ in *tg*; 1.0 mA stimulation), two-way repeated-measures ANOVA failed to show a significant effect of the genotype ($F_{(1,18)} = 3.907$; $p > 0.06$) (Fig. 2*B*).

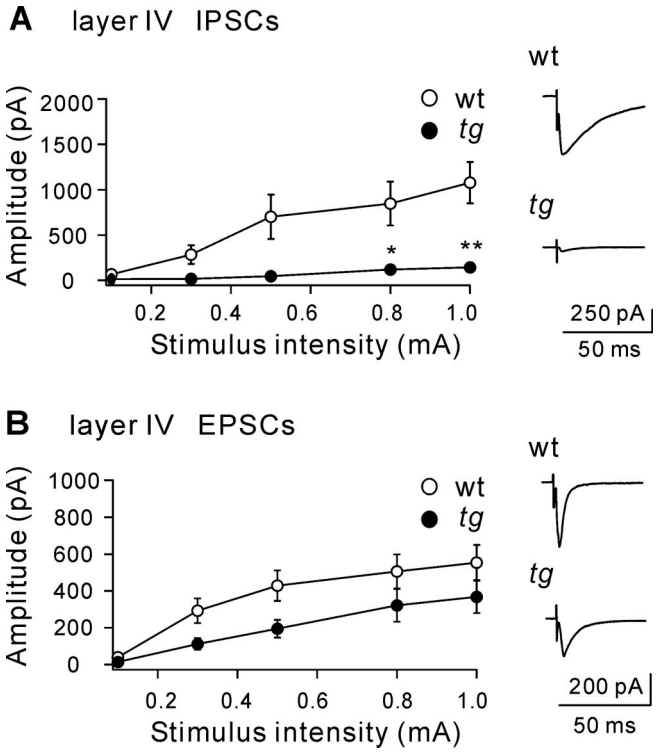

Figure 2. Impaired IPSCs of layer IV pyramidal cells in *tg* mice (P21–P30). IPSCs and EPSCs were evoked by local stimulation in layer IV pyramidal cells in wt and *tg* mice at P21–P30. ***A***, IPSCs were recorded in the presence of CNQX (10 μM) and APV (100 μM). The insets show IPSC traces evoked by 1.0 mA stimulation. The IPSC peak amplitude was plotted against the intensity of stimulation for wt and *tg* mice. The IPSC amplitude was significantly smaller in *tg* mice, and two-way repeated-measures ANOVA revealed a significant effect of the genotype ($p < 0.004$). ***B***, EPSCs were recorded in the presence of bicuculline (10 μM). The insets show EPSC traces evoked by 1.0 mA stimulation. The EPSC amplitudes increased with increment of stimulus intensity in both wt and *tg* mice, and two-way repeated-measures ANOVA failed to show a significant effect of the genotype ($p > 0.06$). $^{*}p < 0.05$ and $^{**}p < 0.01$ indicate significant differences between wt and *tg* mice at each stimulus intensity, by multiple comparisons using Bonferroni's test (no asterisks indicate no significant differences).

To see whether a similar synaptic impairment was observed in other primary sensory cortical areas, we also examined the primary auditory cortex. We recorded IPSCs of pyramidal cells evoked by local stimulation as used in the somatosensory cortex. In both wt ($n = 10$) and *tg* ($n = 10$) mice, locally evoked IPSC amplitudes increased with increments of stimulus intensity. Two-way repeated-measures ANOVA revealed no significant effect of the genotype on layer IV IPSC amplitudes in the primary auditory cortex ($F_{(1,18)} = 0.249$; $p > 0.6$) (supplemental Fig. 1, available at www.jneurosci.org as supplemental material).

Miniature IPSCs in layer IV pyramidal neurons

The responses evoked by local stimulation demonstrated that inhibitory synaptic transmission onto layer IV pyramidal neurons in the somatosensory cortex was drastically impaired in epileptic *tg* mice. The site of the impairment could be presynaptic or postsynaptic. One possibility was that neurotransmitter release from presynaptic terminals was not functional in *tg* mice because of the mutation of the $Ca_V2.1$ channel, although, in a normal condition, local stimulation should evoke neurotransmitter release at a high probability from the synaptic terminals of the

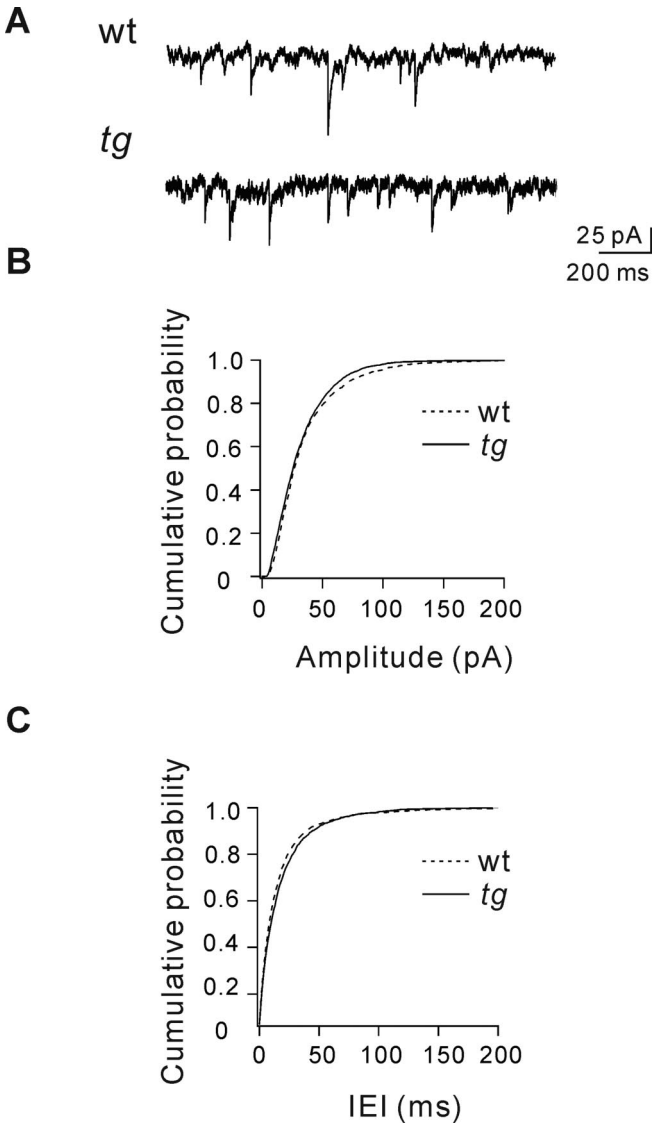

Figure 3. mIPSCs in layer IV pyramidal cells in wt and *tg* mice (P21–P27). mIPSCs were recoded in the presence of TTX (1 μM). ***A***, Traces of mIPSCs recorded in layer IV pyramidal cells of wt (top) and *tg* (bottom) mice. Holding potential −60 mV. ***B***, ***C***, Cumulative distributions of the mIPSC peak amplitude (***B***) and IEI (***C***) of wt and *tg* mice. Number of events was 2800 for each.

thalamocortical projection. The other possibility was that postsynaptic $GABA_A$ receptors were reduced in number or their functional properties were altered in *tg* mice. To examine the two possibilities, mIPSCs were recorded in the presence of CNQX, APV, and TTX (1 μM) (Fig. 3*A*). TTX was used to block voltage-dependent Na^+ channel so that spontaneous firings of neuronal populations were suppressed. The mIPSC amplitude (36.6 ± 0.6 pA, $n = 7$ in wt; 33.0 ± 0.5 pA, $n = 7$ in *tg*) and IEI (17.8 ± 0.5 ms, $n = 7$ in wt; 21.2 ± 0.5 ms, $n = 7$ in *tg*) appeared similar between *tg* and wt mice. However, a statistical test of the cumulative probability distributions (Fig. 3*B*,*C*) showed a significant shift toward smaller amplitudes (Kolmogorov–Smirnov test, $p = 0.002$) and a significant shift toward longer IEIs ($p = 0.001$) in *tg* mice. These results suggested that, although there are slight alterations on the presynaptic (prolonged IEIs) or postsynaptic (reduced mIPSC amplitude) side, these changes could not account for the greatly reduced evoked IPSCs in layer IV pyramidal cells of *tg* mice.

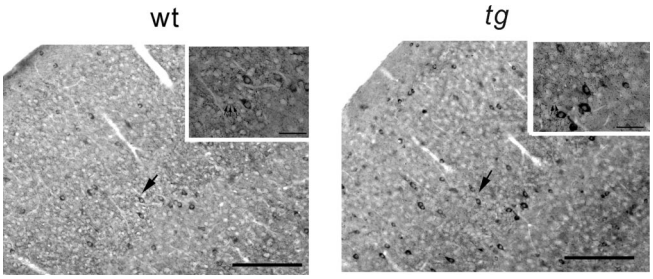

Figure 4. Distribution of inhibitory neurons and their axon terminals in the barrel cortex. Distribution of inhibitory neurons and their axons in the layer IV of the barrel cortex was studied by an immunohistochemical method using anti-GAD antibody. GAD-immunoreactive neurons in wt and *tg* mice (P21–P24). There was no obvious difference in distribution of GAD-immunoreactive neurons between wt and *tg* mice. Arrows point to GAD-immunoreactive neurons. Scale bars, 200 μm. Insets show that punctately stained GAD-immunoreactive axon terminals were observed around somata of large cells (indicated by the arrows). Scale bars, 50 μm.

Number of inhibitory neurons

Another possibility to cause the markedly reduced IPSCs in layer IV was that the number of inhibitory interneurons was reduced in layer IV of *tg* mice. To test this possibility, distribution of inhibitory neurons was analyzed by the immunohistochemical method using polyclonal antibody against GAD (McLaughlin et al., 1975).

There was no obvious difference in the distribution of GAD-immunoreactive cells in the barrel cortex between wt and *tg* mice (Fig. 4). The density of GAD-immunoreactive cells in layer IV showed no statistical difference between wt mice (184 ± 26 cells/mm^2; $n = 5$) and *tg* mice (192 ± 24 cells/mm^2; $n = 5$; $p > 0.05$, *t* test). Cell bodies of large, presumable pyramidal, neurons in layer IV in both wt and *tg* mice were similarly surrounded by immunoreactive GABAergic terminals (Fig. 4, insets, arrows). Furthermore, *tg* mice grow without epilepsy until 3 weeks of age, suggesting that inhibitory neurons and their connections develop normally (see below). Putting all these results together, we concluded that the impaired IPSCs in *tg* mice was caused by functional impairments of neurotransmitter release from the presynaptic nerve terminals.

Layer-specific impairment of IPSCs

Thalamocortical afferents form synapses not only with neuronal elements in layer IV including pyramidal cells (White and Hersch, 1981) but also with corticothalamic pyramidal cells, which are located in lower layer V and upper layer VI and project to the ventrobasal complex of the thalamus (White and Hersch, 1982; White and Keller, 1987). To test whether the impairment of IPSCs was dependent on the laminar position in the somatosensory cortex, locally evoked IPSCs and EPSCs were recorded in layer V pyramidal cells. Different from the layer IV neurons, the reduction in IPSC amplitude was not observed in layer V pyramidal cells in *tg* compared with that of wt mice. IPSC amplitudes with 1.0 mA stimulation were 999 ± 389 pA ($n = 10$) in wt and 1179 ± 312 pA ($n = 10$) in *tg* mice. Two-way repeated-measures ANOVA revealed no significant effect of the genotype ($F_{(1,18)} = 0.236$; $p > 0.6$) (Fig. 5*A*) on layer V IPSC amplitudes.

Conversely, the EPSC amplitude was reduced in layer V pyramidal cells of *tg* mice (392 pA ± 34 pA; $n = 10$, 10 mA stimulation) compared with that of wt mice (615 ± 83 pA; $n = 10$, 10 mA stimulation). Two-way repeated-measures ANOVA showed a significant effect of the genotype ($F_{(1,18)} = 6.100$; $p < 0.03$) (Fig.

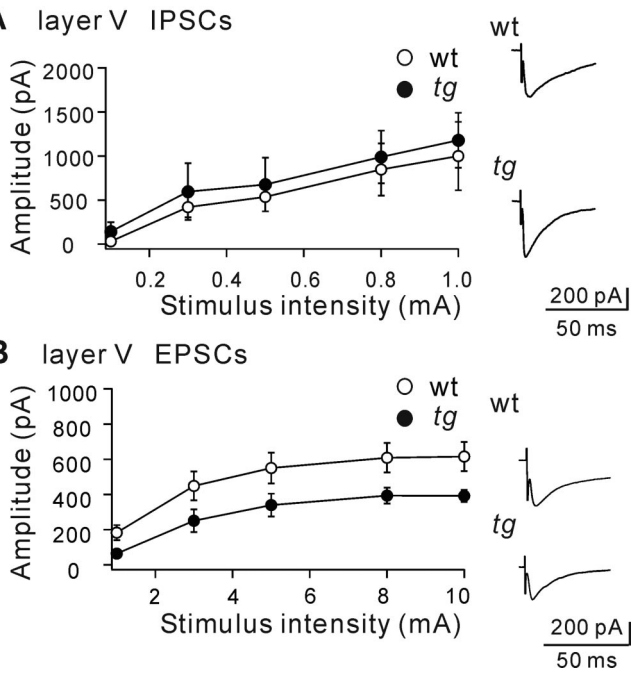

Figure 5. IPSCs recorded in layer V pyramidal cells of wt and *tg* mice (P21–P30). IPSCs and EPSCs evoked by local stimulation were recorded in layer V pyramidal cells of wt and *tg* mice. ***A***, The IPSC peak amplitude was increased with increments of the stimulus intensity in wt and *tg* mice. The insets show IPSC traces by 1.0 mA stimulation. ***B***, The EPSC amplitude in *tg* mice was reduced. The insets show IPSC traces by 10 mA stimulation.

5*B*), but *post hoc* analyses did not show statistical differences between wt and *tg* mice at any stimulus intensities.

Developmental changes in IPSCs

Homozygous *tg* mice develop absence seizures at ~3 weeks of age (Noebels, 1984). If the impairment of IPSCs contributes to the epileptogenesis, the IPSCs may show a related developmental change. To examine this prediction, the developmental effect on the synaptic transmission was studied by comparing nonepileptic young (P14–P16) and epileptic adult (P21–P30) *tg* mice.

In younger mice, the amplitudes of locally evoked IPSCs in layer IV and layer V pyramidal cells were not significantly different between wt and *tg* mice [layer IV, $F_{(1,18)} = 0.351$, $p > 0.5$ (Fig. 6*A*); layer V, $F_{(1,18)} = 1.973$, $p > 0.1$ (Fig. 6*B*)]. Moreover, the evoked EPSC amplitudes in layer IV and layer V were not significantly different in P14–P16 mice [layer IV, $F_{(1,18)} = 0.653$, $p > 0.4$ (Fig. 6*C*); layer V, $F_{(1,18)} = 0.579$, $p > 0.4$ (Fig. 6*D*)]. The IPSC and EPSC amplitudes evoked by maximum stimulation of P14–P16 and P21–P30 mice were summarized in Figure 6*E*. In *tg* mice, the EPSC amplitudes was smaller, but the reduction was not as remarkable as layer IV IPSC reduction at P21–P30.

During the development period from P14–P16 to P21–P30, the IPSC amplitudes of *tg* mice dramatically diminished in the layer IV pyramidal cells (Fig. 6*E*). The IPSC amplitudes in layer V did not show such a developmental change (Fig. 6*E*). These results indicated that the impairment of IPSCs in layer IV was well correlated with the onset of absence seizure.

Developmental switching of Ca^{2+} channel subtypes

The previous studies demonstrated that Ca^{2+} channels involved in neurotransmitter release switch developmentally from the $Ca_V2.2$ (N-type) to $Ca_V2.1$ (P/Q-type) Ca^{2+} channels at various mammalian fast synapses (Iwasaki et al., 2000). Although the contribution of the $Ca_V2.2$ channel to EPSCs in layer IV pyramidal cells of the visual cortex was reported not to change developmentally (Iwasaki et al., 2000), developmental changes in Ca^{2+} channel subtypes of cortical IPSCs were not well investigated. Because the developmental switch usually occurs at ~2 weeks of age, it was expected that the switching from $Ca_V2.2$ to $Ca_V2.1$ Ca^{2+} channel might lead to the impairment of IPSCs in *tg* mice.

Developmental changes in sensitivity of IPSCs to the $Ca_V2.1$ channel-selective blocker ω-Aga-IVA (200 nM) and the $Ca_V2.2$ channel-selective blocker ω-CTx-GVIA (3 μM) were studied in layer IV pyramidal cells of wt mice. At P14–P15, application of ω-Aga-IVA only weakly blocked IPSCs (Fig. 7*A*, left). Subsequent coapplication of ω-CTx-GVIA almost completely blocked the remaining IPSCs. Conversely, at P21–P22, the IPSCs were more strongly reduced by application of ω-Aga-IVA (Fig. 7*B*, left). The ω-Aga-IVA-sensitive fraction of IPSCs was increased from 20 ± 4% at P14–P15 ($n = 7$) to 45 ± 3% at P21–P22 ($n = 7$) (**$p < 0.01$, *t* test). In *tg* mice, however, the developmental change in sensitivity of IPSCs to ω-Aga-IVA was not as evident as in wt (25 ± 4% at P14–P15, $n = 3$; 18 ± 7% at P21–P22, $n = 3$; $p = 0.43$) (Fig. 7*A*,*B*, right). These results demonstrated that, whereas the $Ca_V2.1$ channel plays a minor role in young mice, it plays a predominant role in wt adult mice but not in *tg* adult mice for IPSCs in layer IV pyramidal cells of the somatosensory cortex.

Thalamocortical PSPs in wt and *tg* mice

We finally examined how the IPSC impairment in *tg* mice affects excitability in layer IV pyramidal cells using current-clamp recording (Fig. 8). Mean resting membrane potentials of layer IV pyramidal cells were similar in wt mice (−69.4 ± 1.0 mV; $n = 16$) and *tg* mice (−69.6 ± 0.8 mV; $n = 14$; $p > 0.05$). The intrinsic membrane properties were then examined using negative current injection (−100 pA, 500 ms duration). There were no significant differences between wt and *tg* mice in membrane input resistance (157 ± 5 MΩ, $n = 16$ in wt; 172 ± 9 MΩ, $n = 14$ in *tg*; $p > 0.05$) and membrane time constant (13.9 ± 0.8 ms, $n = 16$ in wt; 12.9 ± 0.9 ms, $n = 14$ in *tg*; $p > 0.05$) of layer IV pyramidal cells.

We then examined differences in thalamocortical PSPs in layer IV pyramidal cells of wt and *tg* mice (P21–P30) (Fig. 8*A*,*B*). Thalamic stimulation with weak stimulus intensity evoked just EPSPs in layer IV pyramidal cells of both wt and *tg* mice (50 μA in Fig. 8*A*), which was reported previously in wt mice (Beierlein et al., 2003). In wt mice, stronger thalamic stimulation evoked transient (~1 ms) depolarization, followed by long-lasting hyperpolarization in layer IV pyramidal cells (400 μA in Fig. 8*A*, left, *B*, top) because of recruitment of thalamocortical feedforward IPSCs (Agmon and Connors, 1992; Porter et al., 2001). In contrast to wt mice, we found that 400 μA stimulation evoked transient depolarization followed by small but long-lasting depolarization in layer IV pyramidal cells of *tg* mice (Fig. 8*A*, right, *B*, bottom).

The differences in thalamocortical PSPs were then quantified between wt and *tg* mice. The EPSP amplitudes with 50 μA stimulation were not different (4.11 ± 0.90 mV, $n = 10$ in wt; 3.69 ± 0.52 mV, $n = 10$ in *tg*; $p > 0.05$, *t* test). Amplitudes of the early transient depolarization with 400 μA stimulus intensity were also not different (2.76 ± 0.99 mV, $n = 10$ in wt; 2.50 ± 0.43 mV, $n = 10$ in *tg*; $p > 0.05$) (Fig. 8*C*, Peak). However, thalamic stimulation with 400 μA intensity evoked long-lasting hyperpolarization in wt (−1.91 ± 0.84 mV at 40 ms after stimulation; $n = 10$) (Fig. 8*C*) but long-lasting depolarization in *tg* mice (1.16 ± 0.66 mV at 40 ms after stimulation; $n = 10$) (Fig. 8*C*). Two-way repeated-measures ANOVA revealed a remarkable difference in time

course profiles of the thalamocortical PSPs with 400 μA intensity ($F_{(1,18)} = 7.679$; $p < 0.02$) (Fig. 8*C*). Also, there was a significant difference in stimulus intensity profiles of the thalamocortical PSPs at 40 ms after stimulation, revealed by two-way repeated-measures ANOVA ($F_{(1,18)} = 5.515$; $p < 0.03$) (Fig. 8*D*). These results indicated that thalamic inputs preferentially induce long-lasting depolarization in layer IV pyramidal cells of *tg* mice.

Discussion

Absence epilepsy has long been speculated to arise from an aberration of the interplay between the cerebral cortex and the thalamus. In epileptic model animals, there are many reports to study intrinsic and synaptic defects in the thalamus (Caddick et al., 1999; Zhang et al., 2002) and in the cerebral cortex (Di Pasquale et al., 1997). However, there has been no report to examine directly the synaptic transmission between the thalamus and the cortex. In this study, we used thalamocortical slices of *tg* mice, a well known mouse model of absence seizure, and revealed a significant impairment of feedforward inhibition from the thalamus to layer IV of the somatosensory cortex (Figs. 1, 8).

Layer IV inhibitory synapses dysfunction in epileptic *tg* mice

Our principal finding of this study was a significant reduction (87%) in the amplitude of locally evoked IPSCs, but not that of EPSCs, in layer IV pyramidal cells located in the somatosensory cortex of epileptic *tg* mice. Similar results were obtained with the thalamocortical responses.

To identify the mechanism of the IPSC amplitude reduction, we made several experiments and obtained the following results. (1) GAD-immunoreactive inhibitory neurons were not decreased in number in layer IV of *tg* mice, and GAD-immunoreactive nerve terminals were well observed around presumable pyramidal cells. (2) mIPSCs could be recorded in layer IV pyramidal cells of *tg* mice. Although the amplitude was smaller and interevent interval was prolonged in *tg* mice, these changes were relatively mild. These results suggested that the postsynaptic apparatus was, at least, functional. (3) IPSCs once normally developed in younger mice, but IPSCs became impaired in later developmental stages, when the inhibitory synaptic transmission to layer IV pyramidal cells became more dependent on the $Ca_V2.1$ channel. All of these results suggest that significant impairment of inhibitory synaptic transmission in layer IV pyramidal neurons was not caused by failure of wiring or synapse formation but was caused primarily by dysfunction of neurotransmitter release from presynaptic terminals. Our results, however, do not exclude involvement of secondary effects of the mutation in the pathogenesis of absence seizures, because imbalance of excitation and inhibition could lead indirectly to subtle developmental rearrangements in the number or placement of synaptic inputs.

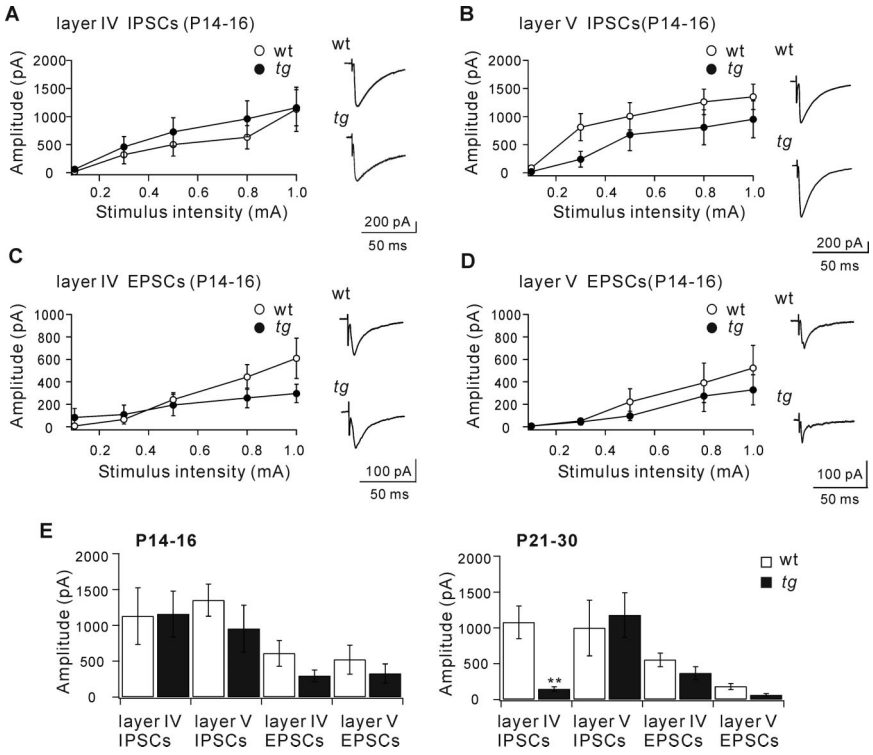

Figure 6. IPSCs and EPSCs in layer IV and V pyramidal cells of younger wt and *tg* mice (P14–P16). ***A–D***, The IPSC and EPSC peak amplitudes of layer IV (***A***, ***C***) and V (***B***, ***D***) were plotted against the intensity of stimulation for wt and *tg* mice at P14–P16. In both layers, the IPSC and EPSC peak amplitudes increased with increments of stimulus intensity in wt and *tg* mice. The insets show IPSC and EPSC traces by 1.0 mA stimulation. ***E***, Averaged IPSC and EPSC peak amplitudes evoked by 1.0 mA stimulation in P14–P16 (left) and P21–P30 (right) mice. All data are represented as mean ± SEM for $n = 10$. $^{**}p < 0.01$, Bonferroni's test.

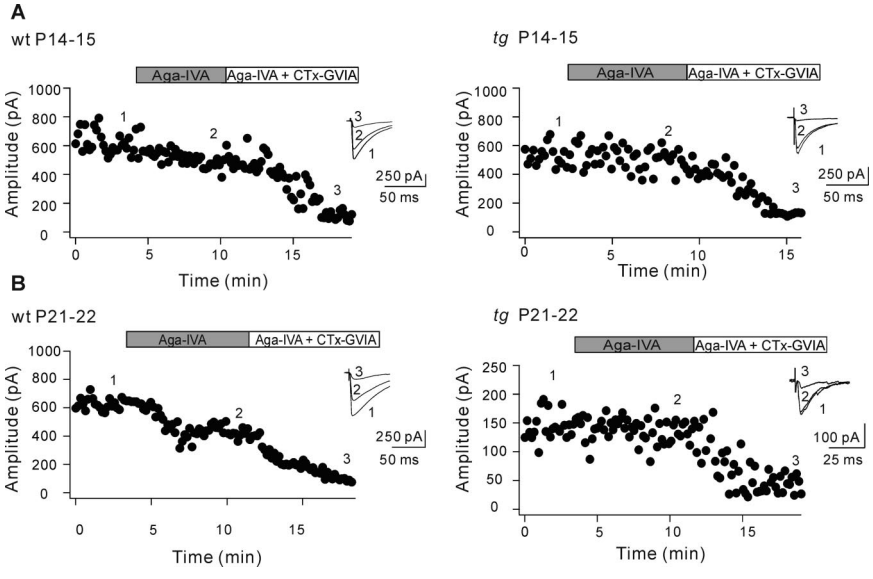

Figure 7. Developmental changes in ω-Aga-IVA sensitivity of IPSCs in layer IV pyramidal cells. ***A***, ***B***, Time course of the peak IPSC amplitude in response to application of ω-Aga-IVA (200 nM; gray bar) and additional ω-CTx-GVIA (3 μM; white bar). The insets show IPSC traces at the time points indicated by the numbers. ω-Aga-IVA reduced the IPSC amplitude by 20% at P14–P15 (***A***, left). ω-Aga-IVA reduced the IPSCs amplitude by 45%, and additional ω-CTx-GVIA almost completely blocked IPSCs at P21–P22 (***B***, left). However, the developmental change of IPSC in ω-Aga-IVA sensitivity was not observed in *tg* mice (***A***, ***B***, right).

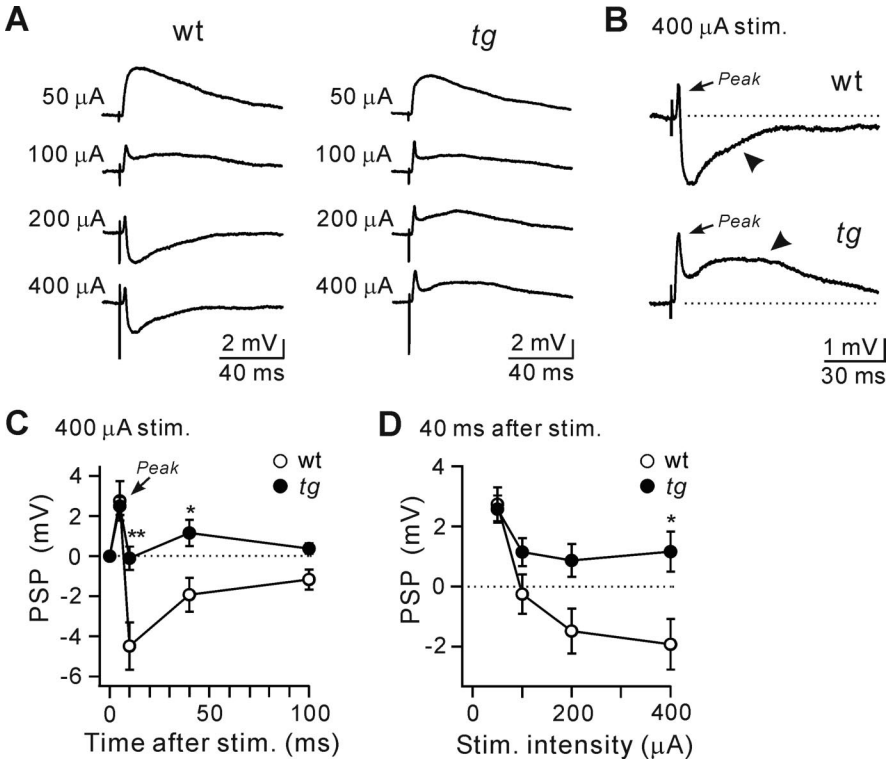

Figure 8. Postsynaptic potentials in layer IV pyramidal cells in response to thalamic stimulation. ***A***, Typical responses of the thalamocortical PSPs in layer IV pyramidal cells of wt (left) and *tg* (right) mice, with increments of the stimulus intensity. ***B***, Vertical expansion of the thalamocortical PSPs with the 400 μA stimulus intensity, which are identical to those in ***A***. Note that the thalamic stimulation with 400 μA intensity evoked transient depolarization followed by long-lasting hyperpolarization in wt mice (top) but long-lasting depolarization in *tg* mice (bottom). The early transient depolarization is indicated by Peak, whereas the late long-lasting hyperpolarization and depolarization are indicated by arrowheads. The membrane potentials before the stimulation were set to −60 mV by current injection. Stimulus artifacts were truncated. ***C***, Time course profiles of thalamocortical PSPs with 400 μA stimulus intensity in wt and *tg* mice. PSP values were calculated as membrane potentials at each time point after stimulation minus those just before stimulation. Peak amplitudes of the early transient depolarization (indicated by Peak) were searched from 2 to 7 ms after stimulation in individual preparations. The time course profiles were significantly different between wt and *tg* mice ($p < 0.02$, two-way repeated-measures ANOVA). $^{*}p < 0.05$, $^{**}p < 0.01$, Bonferroni's test between genotype at each time point. ***D***, Stimulus intensity profiles of thalamocortical PSPs at 40 ms after stimulation. The stimulus intensity profiles were significantly different between wt and *tg* mice ($p < 0.03$, two-way repeated-measures ANOVA). $^{*}p < 0.05$, $^{**}p < 0.01$, Bonferroni's test between genotypes at each stimulus intensity.

Layer-specific dysfunction of synaptic transmission in *tg* mice

Because the $Ca_V2.1$ channel is the predominant Ca^{2+} channel type in the brain, it was anticipated that some parts of the cerebral cortex were impaired in *tg* mice. In fact, a cortical microdialysis assay showed severely attenuated releases of both glutamate and GABA evoked by high K^+ solution (Ayata et al., 2000). In the present study, our analyses at a finer level revealed that synaptic dysfunctions are relatively confined to specific neuronal populations. The reduction in IPSCs was prominent in layer IV pyramidal cells, but it was not observed in layer V pyramidal cells in *tg* mice. The EPSC amplitude in layer V pyramidal cells was also moderately reduced.

Types and functions of layer IV interneurons

The organization of neocortical circuitry is considerably complicated (for review, see Douglas and Martin, 2004). A simplified diagram shows that layer IV neurons are a main gateway receiving inputs from the thalamus, although they receive strong inputs from neurons in layer VI and other layers. Inhibitory interneurons in layers IV that are activated by the thalamocortical projections are morphologically heterogeneous in terms of their dendrites and axons (Porter et al., 2001). The inhibitory interneurons are often grouped into two types based on the patterns of the intrinsic firing, which are the fast-spiking (FS) cells and the low-threshold-spiking (LTS) cells (Gibson et al., 1999; Beierlein et al., 2000; Amitai et al., 2002). Inputs from thalamocortical relay cells are more selective for FS cells and frequently and strongly excite them (Agmon and Connors, 1991; Porter et al., 2001; Beierlein et al., 2002), whereas the thalamocortical inputs only rarely and weakly excite LTS cells (Gibson et al., 1999). Thus, FS neurons play a dominant role in feedforward inhibition of the thalamocortical projection, and this feedforward inhibition is defective in *tg* mice.

Development-dependent dysfunction of inhibitory synapses

Absence seizure in *tg* mice begins at ~3 weeks of age (Noebels and Sidman, 1979). Inhibitory synaptic transmission in layer IV is intact in nonepileptic young *tg* mice but becomes impaired later. These findings imply a relationship between onset of absence epilepsy and impairment of inhibitory synaptic transmission. The Ca^{2+} channel involved in neurotransmitter release often switches developmentally from the $Ca_V2.2$ (N-type) channel to the $Ca_V2.1$ (P/Q-type) channel at various mammalian fast synapses (Iwasaki et al., 2000). In the present work, the sensitivity of inhibitory synaptic transmission to ω-Aga-IVA increased developmentally in layer IV, indicating the subtype switching. Together, we speculate that the neurological phenotype becomes overt at ~3 weeks through the subtype switching, which makes some groups of synapses more dependent on the $Ca_V2.1$ channel. However, we do not think that subtype switching alone can explain such drastically impaired inhibitory synaptic transmission in the cortical layer IV. Whereas the $Ca_V2.1$-dependent component of the inhibitory synaptic transmission was ~45% in adult wt mice, the IPSC amplitude in layer IV pyramidal cells was more severely reduced in *tg* mice (down to 13%). Other mechanisms, including various secondary effects, also must contribute to the drastic reduction.

Compensation of Ca^{2+} channel subtypes in *tg* mice

For the phenotypic effect of the *tg* mutation, two factors seem to be involved: predominance of the $Ca_V2.1$ channel and compensation by other subtypes. If the $Ca_V2.1$ channel is a trivial component, the mutation will not affect the function. If the compensation is adequate, mutational effects will not appear. Compensatory effects of other Ca^{2+} channel subtypes have been investigated in other synapses of *tg* mice. The hippocampal CA3–CA1 synapses are maintained because of compensatory upregulation of $Ca_V2.2$ (Qian and Noebels, 2000). A similar situation is observed in the neuromuscular junction (Plomp et al., 2000). Conversely, cerebellar Purkinje cells lack an ability of compensation. Our preliminary observation showed a drastic reduction in IPSC amplitude measured in deep cerebellar nucleus neurons

evoked by white matter stimulation (presumably Purkinje axons) (Matsushita and Imoto, 2002). In the present work, we do not know whether the compensatory upregulation of $Ca_V2.2$ occurred in layer IV inhibitory neurons, but it is evident that the upregulation, if any, was insufficient.

These lines of evidence imply that different neuronal types have various capacity of compensatory upregulation of other Ca^{2+} channel subtypes in response to the $Ca_V2.1$ channel impairment, and such a variation may underlie selective vulnerability of certain parts of neuronal networks. Molecular determinants of the compensatory upregulation will be an interesting subject for future studies.

Functional implications

Absence epilepsy is characterized by SWDs in wide cortical areas, whose underlying mechanism involves the thalamocortical circuitry (for review, see Manning et al., 2003). To date, synaptic and intrinsic defects in the thalamocortical circuitry have been extensively studied in *tg* mice. In the thalamus of *tg* mice, there are several studies focusing on the role in the generation of the SWDs of low-voltage-activated T-type Ca^{2+} currents in thalamic relay neurons (Zhang et al., 2002; Song et al., 2004). Defects of synaptic transmission were also reported in the thalamus of *tg* mice (Caddick et al., 1999). In the present study, we found a significant impairment of feedforward inhibitory connection from the thalamus to the input layer of the somatosensory cortex.

The thalamocortical feedforward inhibition is an important determinant of excitability to cortical layer IV neurons. As shown in Figure 8*B*, single thalamic stimulation induced transient (~1 ms) depolarization in layer IV pyramidal cells of wt mice, whereas it induced long-lasting depolarization in layer IV pyramidal cells of *tg* mice, because of the impairment of the feedforward inhibition. The longer depolarization in *tg* mice means that thalamic inputs tend to produce bursting activity in layer IV pyramidal cells. Thus, these results imply that synchronous bursts in thalamic relay cells, observed *in vivo*, may be readily transformed into synchronous bursts in layer IV pyramidal cells of *tg* mice, which could be partially reflected as SWDs in the EEG of the somatosensory cortex.

We found that IPSC impairment was observed in the somatosensory cortex but not in the primary auditory cortex (supplemental Fig. 1, available at www.jneurosci.org as supplemental material). Interestingly, a previous study reported that SWDs first originate in the somatosensory cortex and then rapidly spread to other regions of the cortex in the WAG/Rij rat model of absence seizures (Meeren et al., 2002).

In summary, we demonstrated that the effect of the *tg* mutation was variable depending on neuronal cell types and developmental stages, and that the feedforward inhibition was severely impaired in the somatosensory thalamocortical pathway. Because the *tg* phenotype is expected to arise from a complex pattern of altered transmitter release in the cerebral cortex, the thalamus, and other brain regions, further search for synaptic defects is necessary particularly in synaptic connections directly related to the thalamocortical interplay to understand the pathophysiology of absence epilepsy.

References

Agmon A, Connors BW (1991) Thalamocortical responses of mouse somatosensory (barrel) cortex *in vitro*. Neuroscience 41:365–379.

Agmon A, Connors BW (1992) Correlation between intrinsic firing patterns and thalamocortical synaptic responses of neurons in mouse barrel cortex. J Neurosci 12:319–329.

Amitai Y, Gibson JR, Beierlein M, Patrick SL, Ho AM, Connors BW, Golomb D (2002) The spatial dimensions of electrically coupled networks of interneurons in the neocortex. J Neurosci 22:4142–4152.

Avoli M, Gloor P (1982) Interaction of cortex and thalamus in spike and wave discharges of feline generalized penicillin epilepsy. Exp Neurol 76:196–217.

Ayata C, Shimizu-Sasamata M, Lo EH, Noebels JL, Moskowitz MA (2000) Impaired neurotransmitter release and elevated threshold for cortical spreading depression in mice with mutations in the α1A subunit of P/Q type calcium channels. Neuroscience 95:639–645.

Beierlein M, Gibson JR, Connors BW (2000) A network of electrically coupled interneurons drives synchronized inhibition in neocortex. Nat Neurosci 3:904–910.

Beierlein M, Fall CP, Rinzel J, Yuste R (2002) Thalamocortical bursts trigger recurrent activity in neocortical networks: layer 4 as a frequency-dependent gate. J Neurosci 22:9885–9894.

Beierlein M, Gibson JR, Connors BW (2003) Two dynamically distinct inhibitory networks in layer 4 of the neocortex. J Neurophysiol 90:2987–3000.

Caddick SJ, Wang C, Fletcher CF, Jenkins NA, Copeland NG, Hosford DA (1999) Excitatory but not inhibitory synaptic transmission is reduced in lethargic (*Cacnb4*^{lh}) and tottering (*Cacna1a*^{tg}) mouse thalami. J Neurophysiol 81:2066–2074.

Cruikshank SJ, Rose HJ, Metherate R (2002) Auditory thalamocortical synaptic transmission in vitro. J Neurophysiol 87:361–384.

Di Pasquale E, Keegan KD, Noebels JL (1997) Increased excitability and inward rectification in layer V cortical pyramidal neurons in the epileptic mutant mouse *Stargazer*. J Neurophysiol 77:621–631.

Douglas RJ, Martin KA (2004) Neuronal circuits of the neocortex. Annu Rev Neurosci 27:419–451.

Fletcher CF, Lutz CM, O'Sullivan TN, Shaughnessy Jr JD, Hawkes R, Frankel WN, Copeland NG, Jenkins NA (1996) Absence epilepsy in tottering mutant mice is associated with calcium channel defects. Cell 87:607–617.

Gibson JR, Beierlein M, Connors BW (1999) Two networks of electrically coupled inhibitory neurons in neocortex. Nature 402:75–79.

Gil Z, Amitai Y (1996) Properties of convergent thalamocortical and intracortical synaptic potentials in single neurons of neocortex. J Neurosci 16:6567–6578.

Huda K, Imoto K (2001) Defective feedforward inhibition of thalamocortical integration in tottering epileptic mice. Soc Neurosci Abstr 27:555.5.

Iwasaki S, Momiyama A, Uchitel OD, Takahashi T (2000) Developmental changes in calcium channel types mediating central synaptic transmission. J Neurosci 20:59–65.

Jasper HH, Kershman J (1941) Electroencephalographic classification of the epilepsies. Arch Neurol Psychiatry 45:903–943.

Manning JP, Richards DA, Bowery NG (2003) Pharmacology of absence epilepsy. Trends Pharmacol Sci 24:542–549.

Matsushita K, Imoto K (2002) Unplugged inhibitory synaptic transmission in cerebellar nuclei of Ca^{2+} channel mutant mice. Soc Neurosci Abstr 28:437.4.

McLaughlin BJ, Wood JG, Saito K, Roberts E, Wu JY (1975) The fine structural localization of glutamate decarboxylase in developing axonal processes and presynaptic terminals of rodent cerebellum. Brain Res 85:355–371.

Meeren HK, Pijn JP, Van Luijtelaar EL, Coenen AM, Lopes da Silva FH (2002) Cortical focus drives widespread corticothalamic networks during spontaneous absence seizures in rats. J Neurosci 22:1480–1495.

Mori Y, Friedrich T, Kim MS, Mikami A, Nakai J, Ruth P, Bosse E, Hofmann F, Flockerzi V, Furuichi T, Mikoshiba K, Imoto K, Tanabe T, Numa S (1991) Primary structure and functional expression from complementary DNA of a brain calcium channel. Nature 350:398–402.

Noebels JL (1984) A single gene error of noradrenergic axon growth synchronizes central neurones. Nature 310:409–411.

Noebels JL, Sidman RL (1979) Inherited epilepsy: spike-wave and focal motor seizures in the mutant mouse tottering. Science 204:1334–1336.

Plomp JJ, Vergouwe MN, Van den Maagdenberg AM, Ferrari MD, Frants RR, Molenaar PC (2000) Abnormal transmitter release at neuromuscular junctions of mice carrying the *tottering* α_{1A} Ca^{2+} channel mutation. Brain 123:463–471.

Porter JT, Johnson CK, Agmon A (2001) Diverse types of interneurons generate thalamus-evoked feedforward inhibition in the mouse barrel cortex. J Neurosci 21:2699–2710.

Qian J, Noebels JL (2000) Presynaptic Ca^{2+} influx at a mouse central synapse with Ca^{2+} channel subunit mutations. J Neurosci 20:163–170.

Simons DJ, Woolsey TA (1984) Morphology of Golgi-Cox-impregnated barrel neurons in rat SmI cortex. J Comp Neurol 230:119–132.

Song I, Kim D, Choi S, Sun M, Kim Y, Shin HS (2004) Role of the α1G T-type calcium channel in spontaneous absence seizures in mutant mice. J Neurosci 24:5249–5257.

Steriade M, McCormick DA, Sejnowski TJ (1993) Thalamocortical oscillations in the sleeping and aroused brain. Science 262:679–685.

Wakamori M, Yamazaki K, Matsunodaira H, Teramoto T, Tanaka I, Niidome T, Sawada K, NishizawaY, Sekiguchi N, Mori E, Mori Y, Imoto K (1998) Single tottering mutations responsible for the neuropathic phenotype of the P-type calcium channel. J Biol Chem 273:34857–34867.

Wheeler DB, Randall A, Tsien RW (1994) Roles of N-type and Q-type Ca^{2+} channels in supporting hippocampal synaptic transmission. Science 264:107–111.

White EL, Hersch SM (1981) Thalamocortical synapses of pyramidal cells which project from SmI to MsI cortex in the mouse. J Comp Neurol 198:167–181.

White EL, Hersch SM (1982) A quantitative study of thalamocortical and other synapses involving the apical dendrites of corticothalamic projection cells in mouse SmI cortex. J Neurocytol 11:137–157.

White EL, Keller A (1987) Intrinsic circuitry involving the local axon collaterals of corticothalamic projection cells in mouse SmI cortex. J Comp Neurol 262:13–26.

Zhang Y, Mori M, Burgess DL, Noebels JL (2002) Mutations in high-voltage-activated calcium channel genes stimulate low-voltage-activated currents in mouse thalamic relay neurons. J Neurosci 22:6362–6371.